

# involve

a journal of mathematics

Mathematical modeling of integrin dynamics in initial  
formation of focal adhesions

Aurora Blucher, Michelle Salas,  
Nicholas Williams and Hannah L. Callender





# Mathematical modeling of integrin dynamics in initial formation of focal adhesions

Aurora Blucher, Michelle Salas,  
Nicholas Williams and Hannah L. Callender

(Communicated by Michael Dorff)

Cellular motility is an important function in many cellular processes. Among the key players in cellular movement are transmembrane receptor proteins called integrins. Through the development of a mathematical model we investigate the dynamic relationship between integrins and other molecules known to contribute to initial cellular movement such as extracellular ligands and intracellular adhesion proteins called talin. Gillespie's stochastic simulation algorithm was used for numerical analysis of the model. From our stochastic simulation, we found that most activity in our system happens within the first five seconds. Additionally we found that while ligand-integrin-talin complexes form fairly early in the simulation, they soon disassociate into ligand-integrin or integrin-talin complexes, suggesting that the former tertiary complex is less stable than the latter two complexes. We also discuss our theoretical analysis of the model and share results from our sensitivity analysis, using standardized regression coefficients as measures of output sensitivity to input parameters.

## 1. Introduction

The processes of cellular movement and migration are vital to the performance and maintenance of an individual cell and in turn to the well-being of the larger organism. Embryonic development, the immune system response, and tissue regeneration all require cell motility to progress effectively. Cellular processes that are harmful to the body, such as cancer metastasis, also rely on cell motility [Lauffenburger and Horwitz 1996; Fletcher and Theriot 2004]. Due to the importance of cell motility for proper function of an organism, it is necessary to develop a deeper understanding of the mechanisms involved. One way to do so is through the use of mathematical models, which can provide insight beyond that garnered from traditional experimental methods and techniques.

---

*MSC2010:* primary 92C17, 92C37; secondary 90C31.

*Keywords:* cellular motility, mathematical modeling, focal adhesions, Gillespie's algorithm, integrin receptor, sensitivity analysis.

The process of cell motility can be broken down into four general steps. First, the cell protrudes a thin lamellipodium, a projection of the cell's cytoskeleton, from its leading edge in the desired direction of motion. Next, the lamellipodium attaches to the extracellular matrix through the use of focal adhesions, which are macromolecule assemblies containing integrin receptor proteins, actin, and other linking proteins. Then myosin-II, a motor protein in the cell, causes actin strands to converge, which pulls on the focal adhesions and generates traction. Finally, the traction causes weaker focal adhesions in the rear of the cell to detach and, through the contraction of the actin filaments, moves the cell body forward [Wehrle-Haller 2006; Ananthkrishnan and Ehrlicher 2007].

Our focus is on the development of the focal adhesions in the second step of the motility process. In particular, we seek to model the dynamics of integrins, transmembrane receptor proteins that play a major role in the development of these adhesions [Hynes 1992]. Within each focal adhesion, integrins form mechanical linkages to extracellular signaling molecules called ligands. The number of integrins bound to extracellular ligands as well as to intracellular adhesion proteins is a key factor in determining the strength and duration of the linkages, thus providing a deeper understanding of the overall motility properties of the cell.

Other approaches to modeling and investigating focal adhesions have varied. Some models have compared the strength of a given focal adhesion with the number of ligand-integrin bonds within the adhesion (see, for example, [Gallant and Garcia 2007; Gov 2006; Flaherty et al. 2007]). These models have investigated the forces required to detach the cell from its environment, given the number of ligand-integrin bonds. Other stress-based models, such as [Gallant and Garcia 2007; Cozens-Roberts et al. 1990; Ward and Hammer 1993], show the distribution and total stress in the focal adhesions in relation to time or strain of the integrins. Our model differs from these as it takes into account the initial formation of focal adhesions and the binding interactions between the primary molecules present within a nascent adhesion. This has allowed us to investigate which molecules contribute more and in what manner to the formation and fate of focal adhesions.

As our goal is to model the interactions between integrins and other molecules in a focal adhesion, it is necessary to take into account the likelihood that integrins bind to other molecules. Heterodimeric integrins exist in low-affinity ("inactive") and high-affinity ("active") states, and a variety of molecules from both inside and outside the cell are known to take part in the regulation of these integrin states. Among the most important of these molecules are talin and extracellular ligands [Small et al. 2002; Soll 1995]. Talin, which is an intracellular signaling molecule, can bind to and activate integrins from inside the cell. This activation is known to increase an integrin's affinity for ligands. A ligand binding to an integrin also activates the integrin from the outside of the cell, both providing linkage to the

extracellular matrix and increasing the integrin's affinity for intracellular molecules as well as for other ligands [Cluzel et al. 2005].

This paper is organized as follows. In Section 2 (stochastic simulation), we discuss how we use mass action kinetics and Gillespie's algorithm to model a system involving key molecules participating in the early formation of focal contacts. In Section 4 (numerical results), we discuss our results from the stochastic simulation. In Section 5 (deterministic model), we conduct theoretical analysis on an ordinary differential equations model of our system to check the mathematical relevance of the system. Next, in Section 7 (sensitivity analysis), we discuss parameters which may cause more uncertainty in our model output and would therefore warrant further investigation. We conclude with a discussion and future directions.

## 2. Stochastic simulation

Experiments have indicated that the primary players in early focal adhesion formation include integrins, ligands, and talin [Cluzel et al. 2005]. At present, our model focuses on the initial dynamics between these molecules, as depicted in Figure 1.

Integrins bind with ligands to form integrin-ligand complexes, and conversely, ligand-integrin complexes can dissociate into free ligands and free integrins (see Equation (1)). Similarly, integrins can bind with talin to form integrin-talin complexes, which can then dissociate into free ligands and free talin (Equation (2)).

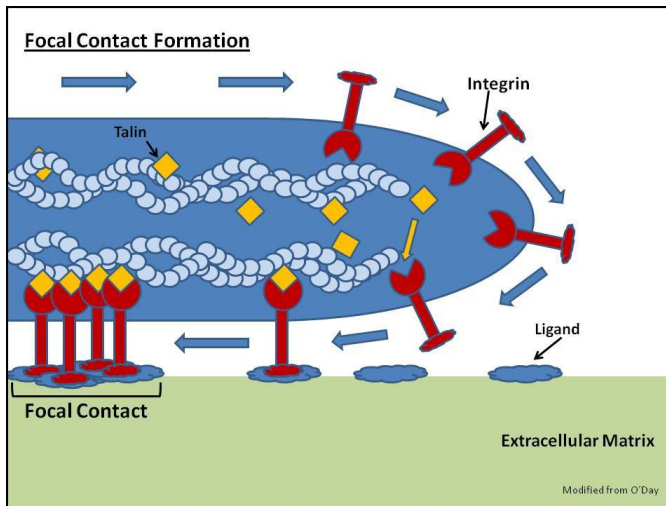


**Figure 1.** Depiction of formation of focal contacts (term commonly used for early focal adhesions) through lateral diffusion of integrins, binding of integrins to talin, and binding of integrins to extracellular ligands. Modified from Figure 12.2 of [O'Day 2012].

Free talin and free ligands can also each bond with complexes from Equations (1) and (2), respectively, to form integrin-ligand-talin complexes, which can then dissociate (Equations (3) and (4)) [Wehrle-Haller 2006]. As integrins are known to diffuse along the plasma membrane, a reaction was also included to allow for the diffusion of integrins into and out of our system, where the diffusing integrins come from an outside source (Equation (5)). Therefore the reactions included in our system are the following:



In the above reactions the following abbreviations are used: L for ligands, I for integrins, LI for ligand-integrin complexes, T for talin, IT for integrin-talin complexes, LIT for ligand-integrin-talin complexes, and S for an outside source of integrins.

Using these reactions, we seek to model the change in the number of each molecule over time. We begin by supposing that the initial number of molecules of each reactant is known. The state vector, denoted by  $X(t)$ , which changes each time one of the above reactions takes place, is used to record the amount of each reactant at any time  $t$ . This state vector evolves according to the propensity functions of our original reactions. The propensity function, denoted by  $a_j$ , is the likelihood that the  $j$ -th reaction will occur and is proportional to the product of the number of molecules of the reactants in the  $j$ -th reaction. For example, take the forward reaction of (1), where ligands bind to integrins with forward rate constant  $k_L^+$ . The propensity function for the forward reaction would be:

$$a_1 = [L] * [I] * k_L^+,$$

where  $[L]$  is the number of free ligand molecules and  $[I]$  of the number of free integrin molecules.

	L	I	IT	LI	LIT	T
$v_1$	-1	-1	0	1	0	0
$v_2$	1	1	0	-1	0	0
$v_3$	0	-1	1	0	0	-1
$v_4$	0	1	-1	0	0	1
$v_5$	-1	0	-1	0	1	0
$v_6$	1	0	1	0	-1	0
$v_7$	0	0	0	-1	1	-1
$v_8$	0	0	0	1	-1	1

**Figure 2.** Stoichiometry matrix.

Next we create a stoichiometry matrix, which is used to track changes in the state vector and allows us to follow changes in the entire system rather than in one reactant. Figure 2 shows the entire stoichiometry matrix. Each row of the matrix tells us which molecules to add, take away, or keep fixed depending on which reaction occurred.

To illustrate how the stoichiometry matrix is used, take the forward reaction of (1), where one ligand and one integrin bind to form a ligand-integrin complex. As shown in Figure 2, the corresponding row for this reaction,  $v_1$ , has a “-1” in both the ligand and integrin columns to indicate the loss of one of each of these molecules and a “+1” in the ligand-integrin complex column to indicate the gain of one complex. Since the other reactants are unaffected by this reaction, all other entries in this row contain a zero.

In order to predict the future states of the whole system of molecules, we seek to model  $P(X, t)$ , the probability of the system being in a certain state,  $X(t)$ , at a certain point in time,  $t$ . This probability is equal to the probability of moving to that state from a neighboring one, given by  $a_j(X(t) - v_j) \cdot P(X(t) - v_j, t)$ , minus the probability of moving from that state to a neighboring one, given by  $a_j(X(t)) \cdot P(X(t), t)$  multiplied by the time step  $\Delta t$ . In general, for a system with  $M$  reactions, we sum all these probabilities for each of the  $M$  reactions, divide by  $\Delta t$ , and take the limit as  $\Delta t$  approaches zero to obtain the *Chemical Master equation*:

$$\frac{dP(X(t), t)}{dt} = \sum_{j=1}^M (a_j(X(t) - v_j) \cdot P(X(t) - v_j, t)) - a_j(X(t)) \cdot P(X(t), t)$$

which is a set of ordinary differential equations for the probability of the whole system being in a particular state  $X(t)$  at any time  $t$ .

### 3. Simulation method: Gillespie's algorithm

The chemical master equation has continuous time, but the state of the system is updated discretely. This makes it very difficult to obtain an analytic solution. Therefore, we approximate a solution using Gillespie's algorithm [1977], which can be summarized in the following steps:

- (1) Initialize the time  $t = t_0$  and the state of the system  $x = x_0$ .
- (2) Evaluate the propensities for each reaction,  $a_j$ , and the sum of the propensities,  $a_{\text{sum}}$ .
- (3) Randomly choose two numbers from a uniform distribution on  $[0, 1]$ , denoted  $\xi_1$  and  $\xi_2$ .
- (4) In order to obtain the next reaction that will take place, let  $j$  be the smallest integer satisfying  $\sum_{j=1}^M a_j(X(t)) > \xi_1 \cdot a_{\text{sum}}(X(t))$ , where  $a_{\text{sum}}$  is the sum of the propensities.
- (5) Let  $\tau = \ln(1/\xi_2)/a_{\text{sum}}(X(t))$ . This determines the next time a reaction will take place. For more details on the choice of  $\tau$ , see [Gillespie 2007].
- (6) Now that the next time step and reaction have been chosen, update the current time,  $t$ , by changing it to  $t + \tau$ . Similarly, update the current state of the system by setting  $X(t + \tau) = X(t) + \nu_j$ , where  $\nu_j$  is the  $j$ -th row of the stoichiometry matrix.
- (7) Repeat steps (1)–(5) until the desired time course has been reached.

The interested reader may see [Higham 2008] for a more detailed description of Gillespie's method. In the fifth step of the algorithm, the state of the system is updated with the stoichiometry matrix. To illustrate this step, assume the forward reaction of step (1) has been randomly chosen to occur at time  $t^*$ . This reaction corresponds to the first row of the stoichiometry matrix. Therefore, if the current state of our system is  $X(t)$ , then to get the new state of the system,  $\nu_1$  is added to  $X(t)$  to obtain  $X(t^*)$  as follows:

$$X(t) = \begin{array}{cccccc} & \text{L} & \text{I} & \text{IT} & \text{LI} & \text{LIT} & \text{T} \\ \left[ \begin{array}{cccccc} 15 & 10 & 0 & 0 & 0 & 0 \end{array} \right] \end{array}$$

$$\nu_1 = \left[ \begin{array}{cccccc} -1 & -1 & 0 & 1 & 0 & 0 \end{array} \right]$$

$$X(t^*) = \left[ \begin{array}{cccccc} 14 & 9 & 0 & 1 & 0 & 0 \end{array} \right]$$

These steps of the algorithm are repeated until the desired time course is achieved. In the next section, we describe the results obtained from simulations of our model for durations of both five and twenty seconds. We also provide an interpretation for the corresponding outputs in the context of our biological system.



### 4. Numerical results

Our stochastic simulations were run in COMplex PATHway SIMulator (CoPaSi), using Gillespie’s algorithm as described in Section 3 and the rate constants shown in Table 1 on the next page. Rate constants were chosen to reflect values of similar parameters from the literature [Lee et al. 2007; Calderwood et al. 2002] and represent an initial attempt to compare the stochastic and deterministic results. For more details on how CoPaSi implements Gillespie’s method, see [Gibson and Bruck 2000].

Figures 3 and 4 show several examples of CoPaSi output from one simulation. The two graphs in Figure 3 show reactant activity over twenty seconds: the upper graph shows activity for all reactants, while the lower combines all integrin complexes into *bound integrins* (BI). The two graphs in Figure 4 show the same reactant activity over the shorter time course of five seconds.

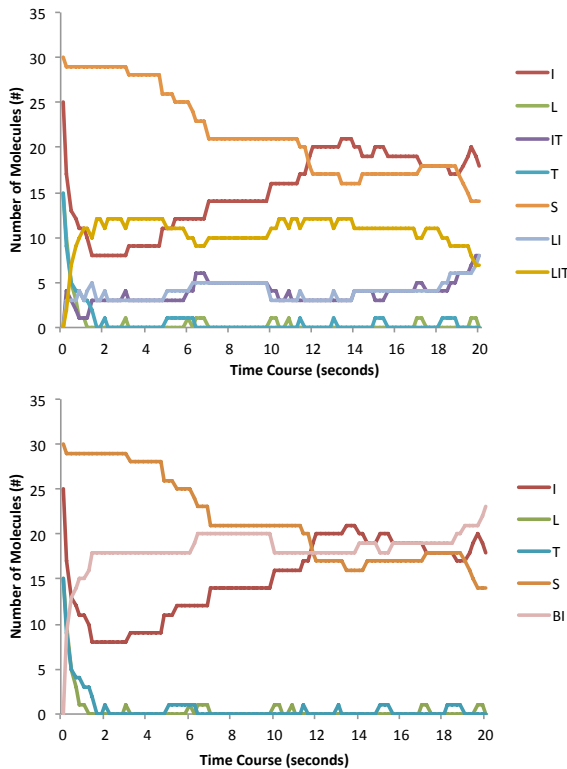


**Figure 3.** Representative output for each model variable, simulated stochastically through Gillespie’s algorithm (described in Section 3) in CoPaSi. Abbreviations are as follows: IT = integrin-talin complex; I = integrin; LIT = ligand-integrin-talin complex; LI = integrin-ligand complex; L = ligand; T = talin; BI = bound integrins (IT + LI + LIT).

Reaction equation	Rate value	Parameter name
$I + L \longrightarrow LI$	0.1	$k_L^+$
$LI \longrightarrow I + L$	0.05	$k_L^-$
$I + T \longrightarrow IT$	0.1	$k_T^+$
$IT \longrightarrow I + T$	0.072	$k_T^-$
$IT + L \longrightarrow LIT$	0.5	$k_{LIT}^+$
$LIT \longrightarrow IT + L$	0.05	$k_{LIT}^-$
$LI + T \longrightarrow LIT$	0.3	$k_{LIT}^+$
$LIT \longrightarrow LI + T$	0.04	$k_{LIT}^-$
$S \longrightarrow I$	0.05	$k_D^+$
$I \longrightarrow S$	0.01	$k_D^-$

**Table 1.** Rate parameters for model reactions.

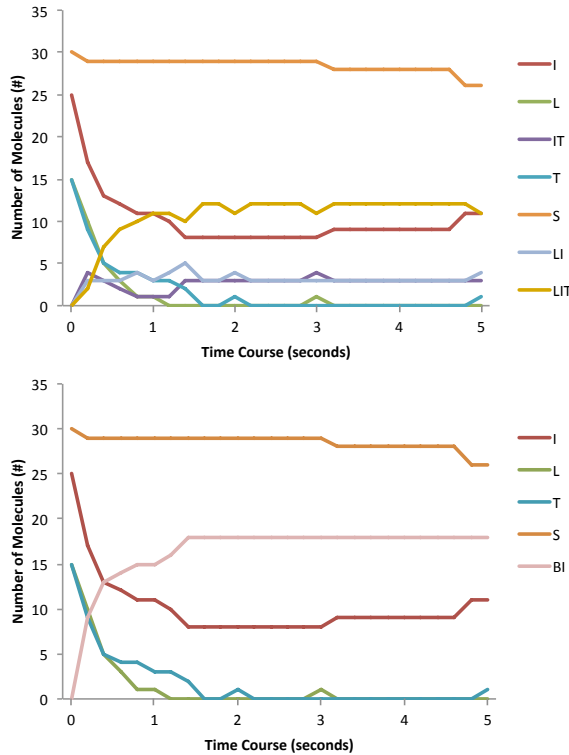


**Figure 4.** Representative output for each model variable, simulated stochastically through Gillespie’s algorithm (described in Section 3) in CoPaSi. Abbreviations are as follows: IT = integrin-talin complex; I = integrin; LIT = ligand-integrin-talin complex; LI = integrin-ligand complex; L = ligand; T = talin; BI = bound integrins (IT + LI + LIT).

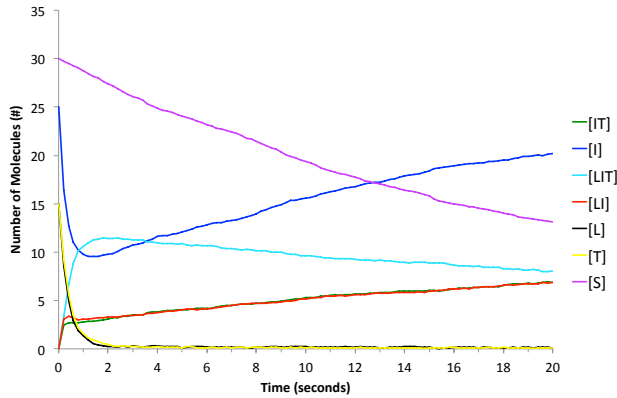


**Figure 5.** The average of 100 stochastic simulations over 20 seconds using Gillespie’s algorithm in CoPaSi. Abbreviations are as follows: IT = integrin-talin complex; I = integrin; LIT = ligand-integrin-talin complex; LI = integrin-ligand complex; L = ligand; T = talin.

Of particular interest is the activity of talin and ligand molecules, which are depleted very early in the simulation (just before 2 seconds have elapsed) and remain very close to zero throughout the time course, with most activity occurring within the first five seconds. The corresponding increases in LI and IT complexes is expected, but the gradual increase in LI and IT and the gradual decrease in LIT complexes indicate that the former two complexes are more stable than the latter. This suggests that while LIT complexes form early on in focal adhesion development, the tertiary complex is less stable and therefore possibly less vital to continued stability of the overall focal adhesion.

While analyzing individual simulations of our stochastic model can provide information on the random interactions of individual species, the average of multiple simulations provides insight into overall trends in the dynamics of our system. As shown in Figure 5, the responses of the reactants averaged over 100 simulations are qualitatively similar to that of a sample individual simulation. Figure 5 also supports the observation from individual simulations that most of the system activity happens within the first five seconds.

Corresponding standard deviations were computed to examine the variability for each reactant in our system. Figure 6 shows the average of 100 simulations and the standard deviation for ligand-integrin-talin complexes and ligands, respectively.

## 5. Deterministic model

For a more thorough investigation of our model, we also looked at the reactions using ordinary differential equations. These equations are based on assumptions

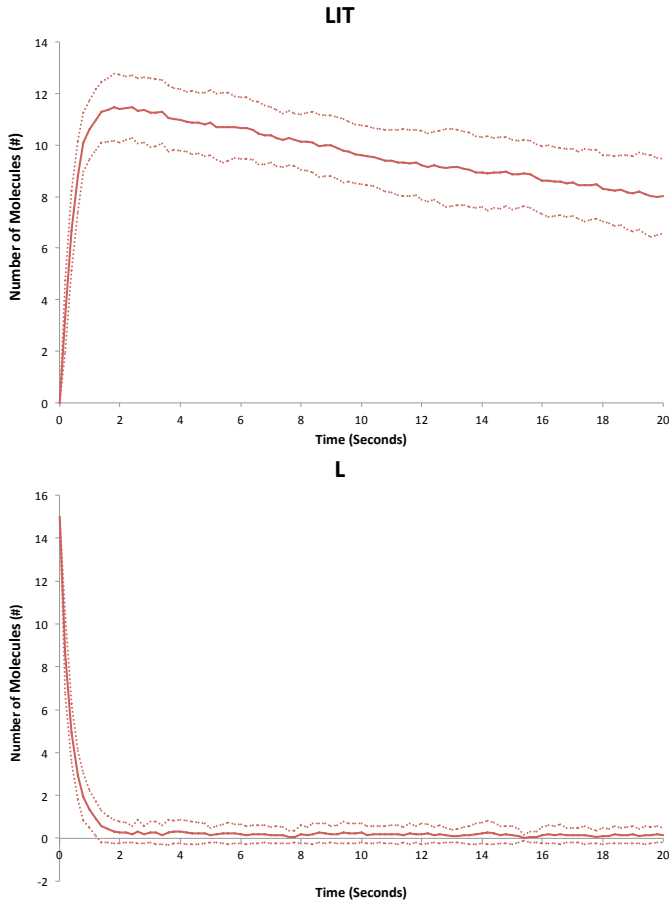


**Figure 6.** The average (in solid lines) of 100 stochastic simulations with one standard deviation from the mean (in dotted lines) for ligand-integrin-talin complexes (top) and free ligands (bottom).

of mass-action kinetics which states that the rate of a chemical reaction is directly proportional to the molecular concentrations or number of molecules of the reacting substances. Take, for example, the forward reaction of (1), where ligands bind with integrins to form ligand-integrin complexes with forward rate constant  $k_L^+$ . Similarly, ligand-integrin complexes dissociate to form free ligands and integrins, with backwards rate constant  $k_L^-$ . However, this is only one of the reactions affecting the amount of free ligands at any time  $t$ . Taking into consideration the other reactions affecting the amount of free ligands, we form the following ordinary differential equation for the change in ligands:

$$\frac{d[L]}{dt} = -k_L^+[L] \cdot [I] + k_L^-[LI] - k_{LT}^+[L] \cdot [IT] + k_{LT}^-[LIT].$$

Note that  $k_L^+$  follows a negative sign since that is the rate at which we lose ligands and integrins, and  $k_L^-$  follows a positive sign because that is the rate at which we lose ligand-integrin complexes and thus gain ligands. We proceed in a similar manner for the rest of the reactions and form our system of ordinary differential equations:

$$\frac{d[L]}{dt} = -k_L^+[L] \cdot [I] + k_L^-[LI] - k_{LT}^+[L] \cdot [IT] + k_{LT}^-[LIT], \quad (6)$$

$$\frac{d[I]}{dt} = -k_L^+[L] \cdot [I] + k_L^-[LI] + k_D^+[S] - k_D^-[I] - k_T^+[T] \cdot [I] + k_T^-[IT], \quad (7)$$

$$\frac{d[LI]}{dt} = k_L^+[L] \cdot [I] - k_L^-[LI] - k_{LIT}^+[T] \cdot [LI] + k_{LIT}^-[LIT], \quad (8)$$

$$\frac{d[IT]}{dt} = k_T^+[T] \cdot [I] - k_T^-[IT] - k_{LT}^+[L] \cdot [IT] + k_{LT}^-[LIT], \quad (9)$$

$$\frac{d[LIT]}{dt} = k_{LT}^+[L] \cdot [IT] - k_{LT}^-[LIT] + k_{LIT}^+[T] \cdot [LI] - k_{LIT}^-[LIT], \quad (10)$$

$$\frac{d[S]}{dt} = k_D^-[I] - k_D^+[S], \quad (11)$$

$$\frac{d[T]}{dt} = -k_T^+[T] \cdot [I] + k_T^-[IT] - k_{LIT}^+[T] \cdot [LI] + k_{LIT}^-[LIT]. \quad (12)$$

Numerical solutions to this system of equations were obtained using the Matlab differential equation solver `ode15s`. The initial conditions were as follows:  $L = 15$ ,  $I = 25$ ,  $IT = 0$ ,  $LI = 0$ ,  $LIT = 0$ ,  $T = 15$ , and  $S = 30$ . The results of the deterministic simulation (Figure 7) are very similar to the average of the results of 100 stochastic simulations (Figure 5). Both graphs show similar behavior for the amounts of all

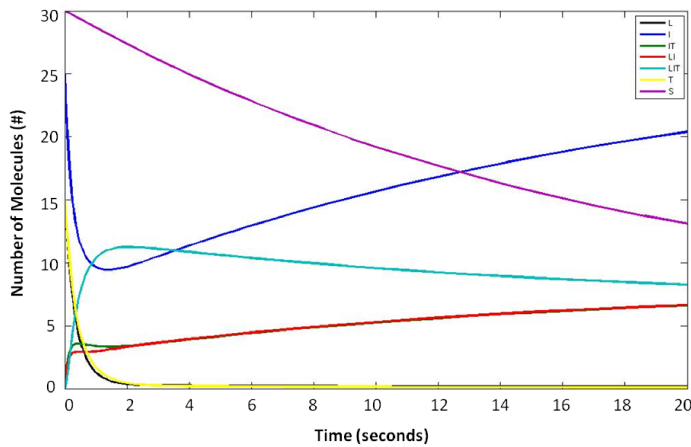


**Figure 7.** Results of deterministic simulation over 20 seconds.

reactants. Additionally, for both the stochastic and the deterministic simulation, the most dynamic behavior occurs within the first five seconds.

## 6. Qualitative analysis

While some systems of equations can be solved analytically, there are many systems for which this cannot be done. Often this is the case for systems of nonlinear equations representing real-world problems, such as complex biological systems. Rather than solving for an analytic solution, or approximating a solution numerically, certain aspects of the solution can be investigated to learn more about the overall qualitative behavior of the system. Among these qualities are existence, uniqueness, boundedness of solutions, and stability of steady state solutions. Due to the wide array of tools available for analysis of deterministic systems, the analysis we have used here is for a deterministic model, rather than a stochastic one.

The first aspect of our solution that we will check is existence. Existence of a solution to our system is important because it enables further model analysis. After verifying existence, we can check our solution for uniqueness. Since we are using deterministic analysis, we should find that our solution is unique, which means that there is exactly one solution for a given set of initial conditions. Biologically, this means that given the same initial amounts of reactants, our system will always behave in the same manner.

In order to show existence of a solution, we use the well-known theorem (stated below) that says that if the right-hand side and the partials of a system of the form  $\dot{x} = f(t, x)$  are continuous in some finite region  $B$ , and also bounded in region  $B$ , then the approximations given in (14) that satisfy the given initial condition in (13) converge uniformly on a given interval of time to a solution of the system.

**Theorem 1** [Brauer and Nohel 1969]. *Let  $f$  and  $\partial f/\partial x_j$  ( $j = 1, \dots, n$ ) be continuous on the box  $B = \{(t, x) : |t - t_0| \leq a, |x - \eta| \leq b\}$ , where  $a$  and  $b$  are positive numbers, and satisfying the bounds*

$$|f(t, x)| \leq N, \quad \left| \frac{\partial f(t, x)}{\partial x_j} \right| \leq K \quad (j = 1, \dots, n),$$

for  $(t, x)$  in  $B$ . Let  $\alpha$  be the smaller of the numbers  $a$  and  $b/N$  and define the successive approximations

$$\phi_0(t) = \eta, \tag{13}$$

$$\phi_n(t) = \eta + \int_{t_0}^t f(s, \phi_{n-1}(s)) ds. \tag{14}$$

Then the sequence  $\phi_j$  of successive approximations converges (uniformly) on the interval  $|t - t_0| \leq \alpha$  to a solution  $\phi(t)$  of the system that satisfies the initial condition  $\phi(t_0) = \eta$ .

We first note that our system is in the form  $\dot{x} = f(t, x)$ , where  $f(t, x)$  is a vector-valued function equal to the right-hand side of our system in (6)–(12). To check that our system satisfies the continuity requirements of the theorem, we check that the right-hand sides of (6)–(12) and all of their partials are continuous. For example, in (6) the right-hand side is composed of positive rate constants multiplied by variables, so it is continuous.

Next we check that the partial derivatives from this equation are continuous. The partial derivative with respect to L is

$$\frac{\partial f}{\partial [L]} = -k_L^+ [I] - k_{LT}^+ [IT].$$

The partial derivative does not contain any terms that could be discontinuous at any point. It can be shown that the partial derivatives with respect to the remaining variables in (6), as well as all partials for the remaining six equations of the system are continuous everywhere. Additionally, it can be seen that both the right-hand side and partial derivatives with respect to each variable in equations (6)–(12) are bounded in finite time. Therefore, the continuity and boundedness requirements have been met for Theorem 1.

The following well-known theorem can now be used to show uniqueness:

**Theorem 2** [Brauer and Nohel 1969]. *Suppose  $f$  and  $\partial f/\partial x_j$  ( $j = 1, \dots, n$ ) are continuous on the box  $B = \{(t, x) : |t - t_0| \leq a, |x - \eta| \leq b\}$ . Then there exists at most one solution of the system satisfying the initial condition  $\phi(t_0) = \eta$ .*

We have previously shown that our system meets both of these requirements, so we now know that our solution exists and is unique on a finite interval of time. In the final section we will discuss our ongoing qualitative analysis efforts.

### 7. Sensitivity analysis

Sensitivity analysis allows us to examine the strength of the relationship between the input parameters and output of our model. This can provide insight into which parameters of our system more strongly effect the model output and are therefore more of a priority when researching experimental values.

For our model, we used the sensitivity analysis method of standardized regression coefficients (SRCs) to determine which parameters have the greatest effect on the output. In this method, a model is represented as a linear model of the following form, shown here for ligands:

$$L_i(t) = b_0(t) + \sum_j b_j(t)m_{ij} + \epsilon_i(t),$$

where  $L_i$  is the linear fit for the  $i$ -th sample for ligands, each  $m_{ij}$  is a value of the sample matrix as described below, each  $b_j$  is a standardized regression coefficient,

and  $\epsilon_i(t)$  is the error. Here,  $i$  is the index for the number of samples taken, and  $j$  is the index for the number of parameters. The larger the absolute value of the  $b_j$ , the more sensitive the model is to the corresponding parameter.

To create our sample matrix, we used the sampling method of Latin Hypercube Sampling. For each parameter in our model, we create an interval containing the nominal value of the parameter, where the right endpoint is 10% higher than the nominal value and the left endpoint is 10% lower. We then divide the interval into subintervals of equal width and randomly choose a subinterval. From within this subinterval a value is randomly chosen and entered into the sample matrix. After this process has been repeated once for each parameter, the first row of the sample matrix has been created. Note that the sample matrix entry denoted by  $m_{ij}$  represents the value of the  $j$ -th parameter for the  $i$ -th sample. For the next sample, we exclude subintervals from which values have previously been chosen. We continue sampling until only one subinterval remains for each parameter, from which we pick the value for our final sample. The end result is an  $i$  by  $j$  matrix where each row is used to create a linear, time-dependent function for each variable being modeled. This method of sampling ensures that an accurate sampling of the entire interval is obtained, while also allowing for all parameters to change simultaneously through each run.

## 8. Sensitivity analysis results

Standardized regression coefficient values above zero indicate a positive relationship between a particular rate parameter and the amount of a given reactant, where an increase in the rate parameter results in an increase in the amount of the reactant. SRC values below zero indicate a negative relationship, where an increasing value of the rate parameter results in a decrease in the amount of the reactant. The  $R^2$  value is the correlation coefficient associated with using standardized regression coefficients to determine which parameters have a stronger effect on the output of our model. For all seven of our reactants, the  $R^2$  values for the SRCs were well above 0.95 for the time-course of interest and thus the results obtained from our sensitivity analysis are statistically valid. Table 2 provides an overview of the most influential parameters for each model reactant, while the discussion that follows provides an in-depth analysis of the sensitivity results for each reactant in the model.

**SRCs for ligands.** For ligands, all rate parameters have a greater effect for the first five seconds of the simulation, after which the value for each rate parameter levels off. This would seem to indicate that the amount of ligands in our system depends on the early activity of the simulation. In particular, the rate constant  $k_L^+$ , which is the rate at which ligands and integrins bind to form ligand-integrin complexes, has the largest negative effect in the first five seconds on the number of ligands. As



$k_L^+$  increases, it becomes more likely that ligands will bind with integrins to form ligand-integrin complexes, and therefore the number of free ligands will decrease.

**SRCs for integrins.** Two rate parameters in particular have an increasing effect on the amount of integrins:  $k_D^+$ , the rate at which integrins diffuse into the system, and  $k_D^-$ , the rate at which integrins diffuse out of the system. It is interesting to note that these parameters have more of an effect as the simulation continues, which suggests that once all the initial integrins are bound, diffusion into and out of the system will be a greater source for additional free integrins than other complexes disassociating to give free integrins. In the future, we would like to examine a more biologically relevant representation of a diffusing integrin source.

**SRCs for ligand-integrin complexes.** For ligand-integrin complexes, two parameters,  $k_L^+$  and  $k_{LIT}^+$  have a greater effect at the beginning of the simulation before leveling off, while the rest of the parameters have a growing effect on the system. In particular,  $k_L^+$ , the rate at which ligands and integrins bind, most likely has a greater effect on the number of ligand-integrin complexes because such complexes are formed from the free ligands and integrins available at the beginning of the simulation. As other reactions occur, however, there are additional ways to form ligand-integrin complexes (such as a ligand-integrin-talin complex disassociating to produce one ligand-integrin complex and one free talin molecule). Thus, the number of ligand-integrin complexes would depend less on  $k_L^+$  as the simulation progresses.

**SRCs for integrin-talin complexes.** The rate parameter  $k_T^+$  has a greater positive effect than any other parameter on integrin-talin complexes at the very beginning of the simulation (until approximately two seconds) but then decreases and levels

Reactant	Positive effect	Negative effect
L	$k_{LT}^-, k_L^-$	$k_L^+, k_T^+$
I	$k_D^+, k_L^-$	$k_D^-, k_{LIT}^-$
LI	$k_{LIT}^-, k_{LT}^-$	$k_L^-, k_T^-$
IT	$k_{LIT}^-, k_{LT}^-$	$k_L^-, k_T^-$
LIT	$k_L^-, k_T^-$	$k_{LIT}^-, k_{LT}^-$
T	$k_{LIT}^-, k_T^-$	$k_T^+, k_L^+$
S	$k_D^-$	$k_D^+$

**Table 2.** Summary of sensitivity analysis results. For each reactant, the two parameters with the strongest positive and negative effects are listed, as determined by standardized regression coefficient values.

off. However, after about five seconds into the simulation,  $k_L^-$  has the greatest negative effect and  $k_{LIT}^-$  has the greatest positive effect on the number of integrin-talin complexes. This suggests that as  $k_L^-$  increases, the number of ligand-integrin complexes decreases, which in turn results in a decrease in the number of ligand-integrin-talin complexes. With fewer LIT complexes to disassociate into free ligands and integrin-talin complexes, there will be a decrease in the number integrin-talin complexes. This illustrates how the rate parameter  $k_L^-$  actually has an indirectly negative effect on the number of integrin-talin complexes.

**SRCs for ligand-integrin-talin complexes.** For ligand-integrin-talin complexes, the rate parameter that has the greatest effect is  $k_{LIT}^-$ , which is the rate at which ligand-integrin-talin complexes disassociate to produce talin molecules and ligand-integrin complexes (Figure 8). Uniquely, the parameter  $k_T^+$ , or the rate at which integrin and talin molecules bind to form integrin-talin complexes, has a positive effect until about two seconds into the simulation, at which point it assumes a negative effect. This could be explained by the fact that while many free talin molecules still exist in the beginning of the simulation,  $k_T^+$  will positively contribute to the number of integrin-talin complexes, which in turn will positively effect the number of ligand-integrin-talin complexes. After all the initial free talin molecules are gone, however, an increase in  $k_T^+$  will mean that any later free talin molecules will be more likely to bind with integrins than other reactants. This will leave very few free talin to bind with ligand-integrin complexes, resulting in an overall decrease in the number of ligand-integrin-talin complexes. Thus, after the point in the simulation where the initial free talin molecules are gone,  $k_T^+$  will indirectly negatively effect the number of ligand-integrin-talin complexes.

**SRCs for talin.** Most rate parameters have a stronger effect on the amount of talin within the first five seconds of the simulation, after which they level off (Figure 8). The rate parameter  $k_T^+$ , which is the rate at which integrins and talin molecules bind, has the greatest negative effect during the first five seconds. It is interesting to note here that we might expect the parameter  $k_{LIT}^+$ , or the rate at which ligand-integrin complexes and talin molecules bind to form ligand-integrin-talin complexes, to have a greater effect on the number of talin molecules. However, while  $k_{LIT}^+$  does have a reasonable negative effect, it is overshadowed by the negative effect of  $k_T^+$ . This reflects the earlier inference that as  $k_T^+$  is increased, there is a decrease in the amount of ligand-integrin-talin complexes.

**SRCs for diffusing integrins.** For the amount of diffusing integrins, the only rate parameters that have an effect are  $k_D^+$  and  $k_D^-$ . This is reasonable given that the only reaction these integrins are involved in is either diffusion into the system or diffusion out of the system. Thus, the number of integrins in the pool outside of the system is entirely dependent on the rate at which integrins both leave and return to the pool.

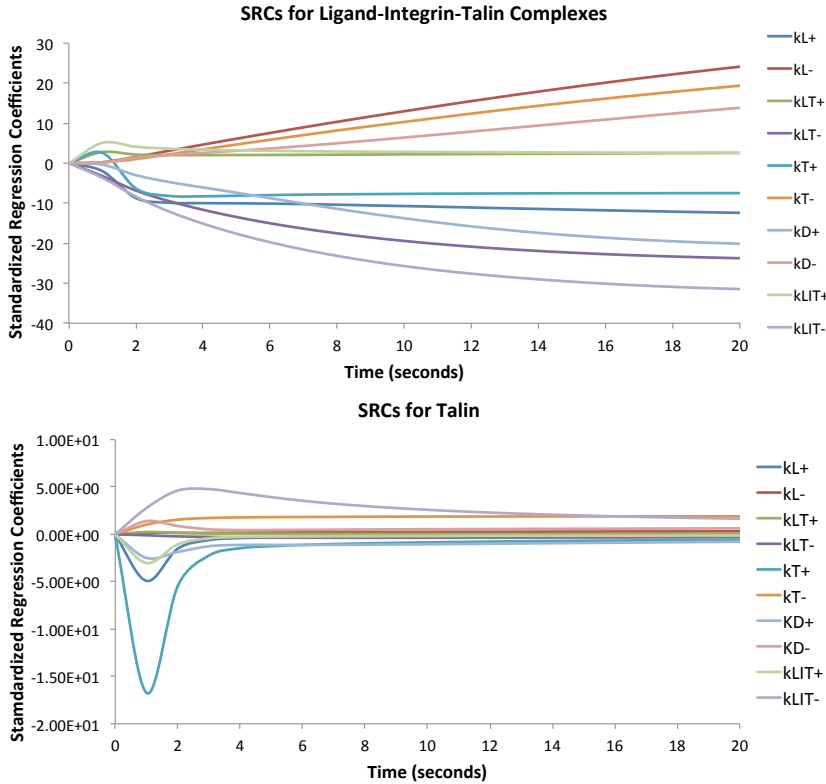


**Figure 8.** Standardized regression coefficients for ligand-integrin-talin complexes (top) and free talin molecules (bottom) in the system over a time period of 20 seconds.

### 9. Conclusion and future work

The averaged results of our stochastic simulations are similar to the results from our deterministic simulation, with both simulation types indicating that initial focal adhesion formation occurs rapidly. This makes sense biologically because a motile cell receiving outside signaling would likely be required to react quickly in response. However, the speed of focal adhesion formation still needs to be determined experimentally, and our model only offers a possible outcome of such experiments.

The first step for future qualitative analysis for our system will be to demonstrate boundedness of our solutions. Boundedness of solutions is an important aspect to check given the context of our model. For instance, it would not make sense if we discovered that a solution approached infinity in finite time or attained negative values, since our system is modeling finite numbers of molecules over time. Additionally, the steady-state solutions to the system can be solved for, and

investigation can be conducted as to local and global stability of these steady-state solutions.

While the sensitivity analysis is a good start in analyzing how sensitive the model is to different parameters, a more accurate assessment could be accomplished with additional rate values from the literature. Additional methods of sensitivity analysis could shed more light on how the rate parameters affect the simulation output. These methods include factors prioritization, which would pinpoint the most influential factors in our system, and the Method of Morris, which would identify factors with negligible effects and allow us to narrow our focus. While the sensitivity analysis conducted thus far is only for the deterministic model, methods for sensitivity analysis of stochastic models are currently being investigated and are an area for future work.

In the future, we would like to find more accurate values from the literature for the rate parameters in our model, beginning with the parameters to which our model output is most sensitive, as indicated by our sensitivity analysis. We would also like to include additional molecules involved in focal adhesion formation, such as PIP<sub>2</sub>, which increases the affinity of talin for integrins. We could then see if we retain a longer period of dynamic behavior in our stochastic results compared to our deterministic results. Additionally, we would like to allow for the diffusion of molecules other than integrins in and out of our system. This could result in more activity within our system as molecules are replenished.

### Acknowledgements

We would like to thank the Center for Undergraduate Research in Mathematics for their financial support of this work through an NSF grant (DMS-063664).

### References

- [Ananthkrishnan and Ehrlicher 2007] R. Ananthkrishnan and A. Ehrlicher, “The forces behind cell movement”, *Int. J. Biol. Sci.* **3**:5 (2007), 303–317.
- [Brauer and Nohel 1969] F. Brauer and J. A. Nohel, *The qualitative theory of ordinary differential equations: an introduction*, W. A. Benjamin, New York, 1969. Reprinted Dover, New York, 1989. Zbl 0179.13202
- [Calderwood et al. 2002] D. A. Calderwood, B. Yan, J. M. de Pereda, B. G. Alvarez, Y. Fujioka, R. C. Liddington, and M. H. Ginsberg, “The phosphotyrosine binding-like domain of talin activates integrins”, *J. Biol. Chem.* **277**:24 (2002), 21749–21758.
- [Cluzel et al. 2005] C. Cluzel, F. Saltel, J. Lussi, F. Puhle, B. A. Imhof, and B. Wehrle-Haller, “The mechanisms and dynamics of avb3 integrin clustering in living cells”, *J. Cell Biol.* **171**:2 (2005), 383–392.
- [Cozens-Roberts et al. 1990] C. Cozens-Roberts, D. A. Lauffenburger, and J. A. Quinn, “Receptor-mediated cell attachment and detachment kinetics”, *J. Biophys.* **58** (1990), 841–856.

- [Flaherty et al. 2007] B. Flaherty, J. P. McGarry, and P. E. McHugh, “Mathematical models of cell motility”, *Cell Biochem. Biophys.* **49** (2007), 14–28.
- [Fletcher and Theriot 2004] D. A. Fletcher and J. A. Theriot, “An introduction to cell motility for the physical scientist”, *Phys. Biol.* **1**:1 (2004).
- [Gallant and Garcia 2007] N. D. Gallant and A. J. Garcia, “Model of integrin-mediated cell adhesion strengthening”, *J. Biomech.* **40** (2007), 1301–1309.
- [Gibson and Bruck 2000] M. A. Gibson and J. Bruck, “Efficient exact stochastic simulation of chemical systems with many species and many channels”, *J. Phys. Chem. A* **104**:9 (2000), 1876–1889.
- [Gillespie 1977] D. T. Gillespie, “Exact stochastic simulation of coupled chemical reactions”, *J. Phys. Chem.* **81**:25 (1977), 2340–2361.
- [Gillespie 2007] D. T. Gillespie, “Stochastic simulation of chemical kinetics”, *Annu. Rev. Phys. Chem.* **58**:1 (2007), 35–55.
- [Gov 2006] N. S. Gov, “Modeling the size distribution of focal adhesions”, *Biophys. J.* **91** (2006), 2844–2847.
- [Higham 2008] D. J. Higham, “Modeling and simulating chemical reactions”, *SIAM Rev.* **50**:2 (2008), 347–368. MR 2009f:80015 Zbl 1144.80011
- [Hynes 1992] R. O. Hynes, “Integrins : versatility, modulation, and signaling in cell adhesion”, *Cell* **69**:1 (1992), 11–25.
- [Lauffenburger and Horwitz 1996] D. A. Lauffenburger and A. F. Horwitz, “Cell migration: a physically integrated molecular process”, *Cell* **84**:3 (1996), 359–369.
- [Lee et al. 2007] C. K. Lee, Y. M. Wang, L. S. Huang, and S. Lin, “Atomic force microscopy: determination of unbinding force, off rate and energy barrier for protein–ligand interaction”, *Micron* **38**:5 (2007), 446–461.
- [O’Day 2012] D. O’Day, *Human cell biology*, eBookIt.com, 2012.
- [Small et al. 2002] J. V. Small, T. Stradal, E. Vignal, and K. Rottner, “The lamellipodium: where motility begins”, *Trends Cell Biol.* **12**:3 (2002), 112–120.
- [Soll 1995] D. R. Soll, “The use of computers in understanding how animal cells crawl”, *Int. Rev. Cytol.* **163** (1995), 43–104.
- [Ward and Hammer 1993] M. D. Ward and D. A. Hammer, “A theoretical analysis for the effect of focal contact formation on cell-substrate attachment strength”, *J. Biophys.* **64** (1993), 936–959.
- [Wehrle-Haller 2006] B. Wehrle-Haller, “The role of integrins in cell migration”, in *Integrins and development*, edited by E. H. J. Danen, Landes Bioscience, Austin, TX, 2006. Madame Curie Biosci. Database.

Received: 2013-01-08      Revised: 2013-08-25      Accepted: 2013-08-29

blucher@ohsu.edu      *Department of Mathematics, University of Portland, 5000  
N. Willamette Boulevard, Portland, OR 97203, United States*

salas11@up.edu      *Department of Biology, University of Portland, 5000  
N. Willamette Boulevard, Portland, OR 97203, United States*

williams13@up.edu      *School of Engineering, University of Portland, 5000  
N. Willamette Boulevard, Portland, OR 97203, United States*

callende@up.edu      *Department of Mathematics, University of Portland, 5000  
N. Willamette Boulevard, Portland, OR 97203, United States*



# involve

msp.org/involve

## EDITORS

### MANAGING EDITOR

Kenneth S. Berenhaut, Wake Forest University, USA, berenhks@wfu.edu

### BOARD OF EDITORS

Colin Adams	Williams College, USA colin.c.adams@williams.edu	David Larson	Texas A&M University, USA larson@math.tamu.edu
John V. Baxley	Wake Forest University, NC, USA baxley@wfu.edu	Suzanne Lenhart	University of Tennessee, USA lenhart@math.utk.edu
Arthur T. Benjamin	Harvey Mudd College, USA benjamin@hmc.edu	Chi-Kwong Li	College of William and Mary, USA ckli@math.wm.edu
Martin Bohner	Missouri U of Science and Technology, USA bohner@mst.edu	Robert B. Lund	Clemson University, USA lund@clemson.edu
Nigel Boston	University of Wisconsin, USA boston@math.wisc.edu	Gaven J. Martin	Massey University, New Zealand g.j.martin@massey.ac.nz
Amarjit S. Budhiraja	U of North Carolina, Chapel Hill, USA budhiraj@email.unc.edu	Mary Meyer	Colorado State University, USA meyer@stat.colostate.edu
Pietro Cerone	La Trobe University, Australia P.Cerone@latrobe.edu.au	Emil Minchev	Ruse, Bulgaria eminchev@hotmail.com
Scott Chapman	Sam Houston State University, USA scott.chapman@shsu.edu	Frank Morgan	Williams College, USA frank.morgan@williams.edu
Joshua N. Cooper	University of South Carolina, USA cooper@math.sc.edu	Mohammad Sal Moselehian	Ferdowsi University of Mashhad, Iran moslehian@ferdowsi.um.ac.ir
Jem N. Corcoran	University of Colorado, USA corcoran@colorado.edu	Zuhair Nashed	University of Central Florida, USA znashed@mail.ucf.edu
Toka Diagana	Howard University, USA tdiagana@howard.edu	Ken Ono	Emory University, USA ono@mathcs.emory.edu
Michael Dorff	Brigham Young University, USA mdorff@math.byu.edu	Timothy E. O'Brien	Loyola University Chicago, USA tobrie1@luc.edu
Sever S. Dragomir	Victoria University, Australia sever@matilda.vu.edu.au	Joseph O'Rourke	Smith College, USA orourke@cs.smith.edu
Behrouz Emamizadeh	The Petroleum Institute, UAE bemamizadeh@pi.ac.ae	Yuval Peres	Microsoft Research, USA peres@microsoft.com
Joel Foisy	SUNY Potsdam foisyjs@potsteam.edu	Y.-F. S. Pétermann	Université de Genève, Switzerland petermann@math.unige.ch
Errin W. Fulp	Wake Forest University, USA fulp@wfu.edu	Robert J. Plemmons	Wake Forest University, USA rplemmons@wfu.edu
Joseph Gallian	University of Minnesota Duluth, USA jgallian@d.umn.edu	Carl B. Pomerance	Dartmouth College, USA carl.pomerance@dartmouth.edu
Stephan R. Garcia	Pomona College, USA stephan.garcia@pomona.edu	Vadim Ponomarenko	San Diego State University, USA vadim@sciences.sdsu.edu
Anant Godbole	East Tennessee State University, USA godbole@etsu.edu	Bjorn Poonen	UC Berkeley, USA poonen@math.berkeley.edu
Ron Gould	Emory University, USA rg@mathcs.emory.edu	James Propp	U Mass Lowell, USA jpropp@cs.uml.edu
Andrew Granville	Université Montréal, Canada andrew@dms.umontreal.ca	József H. Przytycki	George Washington University, USA przytyck@gwu.edu
Jerrold Griggs	University of South Carolina, USA griggs@math.sc.edu	Richard Rebarber	University of Nebraska, USA rrebarbe@math.unl.edu
Sat Gupta	U of North Carolina, Greensboro, USA sngupta@uncg.edu	Robert W. Robinson	University of Georgia, USA rwr@cs.uga.edu
Jim Haglund	University of Pennsylvania, USA jhaglund@math.upenn.edu	Filip Saidak	U of North Carolina, Greensboro, USA f_saidak@uncg.edu
Johnny Henderson	Baylor University, USA johnny_henderson@baylor.edu	James A. Sellers	Penn State University, USA sellersj@math.psu.edu
Jim Hoste	Pitzer College jhoste@pitzer.edu	Andrew J. Sterge	Honorary Editor andy@ajsterge.com
Natalia Hritonenko	Prairie View A&M University, USA nahritonenko@pvamu.edu	Ann Trenk	Wellesley College, USA atrenk@wellesley.edu
Glenn H. Hurlbert	Arizona State University, USA hurlbert@asu.edu	Ravi Vakil	Stanford University, USA vakil@math.stanford.edu
Charles R. Johnson	College of William and Mary, USA crjohnso@math.wm.edu	Antonia Vecchio	Consiglio Nazionale delle Ricerche, Italy antonia.vecchio@cnrit
K. B. Kulasekera	Clemson University, USA kk@ces.clemson.edu	Ram U. Verma	University of Toledo, USA verma99@msn.com
Gerry Ladas	University of Rhode Island, USA gladas@math.uri.edu	John C. Wierman	Johns Hopkins University, USA wierman@jhu.edu
		Michael E. Zieve	University of Michigan, USA zieve@umich.edu

## PRODUCTION

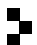
Silvio Levy, Scientific Editor

See inside back cover or [msp.org/involve](http://msp.org/involve) for submission instructions. The subscription price for 2014 is US \$120/year for the electronic version, and \$165/year (+\$35, if shipping outside the US) for print and electronic. Subscriptions, requests for back issues from the last three years and changes of subscribers address should be sent to MSP.

Involve (ISSN 1944-4184 electronic, 1944-4176 printed) at Mathematical Sciences Publishers, 798 Evans Hall #3840, c/o University of California, Berkeley, CA 94720-3840, is published continuously online. Periodical rate postage paid at Berkeley, CA 94704, and additional mailing offices.

Involve peer review and production are managed by EditFLOW<sup>®</sup> from Mathematical Sciences Publishers.

PUBLISHED BY

 **mathematical sciences publishers**  
nonprofit scientific publishing

<http://msp.org/>

© 2014 Mathematical Sciences Publishers

# involve

2014

vol. 7

no. 4

Whitehead graphs and separability in rank two	431
MATT CLAY, JOHN CONANT AND NIVETHA RAMASUBRAMANIAN	
Perimeter-minimizing pentagonal tilings	453
PING NGAI CHUNG, MIGUEL A. FERNANDEZ, NIRALEE SHAH, LUIS SORDO VIEIRA AND ELENA WIKNER	
Discrete time optimal control applied to pest control problems	479
WANDI DING, RAYMOND HENDON, BRANDON CATHEY, EVAN LANCASTER AND ROBERT GERMICK	
Distribution of genome rearrangement distance under double cut and join	491
JACKIE CHRISTY, JOSH MCHUGH, MANDA RIEHL AND NOAH WILLIAMS	
Mathematical modeling of integrin dynamics in initial formation of focal adhesions	509
AURORA BLUCHER, MICHELLE SALAS, NICHOLAS WILLIAMS AND HANNAH L. CALLENDER	
Investigating root multiplicities in the indefinite Kac–Moody algebra $E_{10}$	529
VICKY KLIMA, TIMOTHY SHATLEY, KYLE THOMAS AND ANDREW WILSON	
On a state model for the $SO(2n)$ Kauffman polynomial	547
CARMEN CAPRAU, DAVID HEYWOOD AND DIONNE IBARRA	
Invariant measures for hybrid stochastic systems	565
XAVIER GARCIA, JENNIFER KUNZE, THOMAS RUDELIUS, ANTHONY SANCHEZ, SIJING SHAO, EMILY SPERANZA AND CHAD VIDDEN	

